

EXPERIMENTAL MEASUREMENTS OF ^{99}Tc AND ^{129}I TRANSMUTATION IN TARC AT CERN

E. González on behalf of the TARC collaboration
CIEMAT, Dept. Nuclear Fission, Avda. Complutense 22 Edif. 17
28040 Madrid,
Spain

The TARC collaboration

A. Abánades^{n,(§)}, J. Aleixandre^b, S. Andriamonje^{c,a}, A. Angelopoulos^j, A. Apostolakis^j,
H. Arnould^a, E. Belle^g, C.A. Bompas^a, L. Brillard^f, J. Bueno^b, S. Buono^{c,h,(†)}, F. Carminati^c,
F. Casagrande^{c,e,(¶)}, P. Cennini^c, J.I. Collar^c, E. Cerro^b, R. Del Moral^a, S. Díez^{m,(§)}, L. Dumps^c,
C. Eleftheriadis^l, M. Embid^{i,d}, R. Fernández^{c,d}, J. Gálvezⁱ, J. García^{n,d}, C. Gelès^c, A. Giorni^g,
E. González^{c,d}, O. González^b, I. Goulas^c, D. Heuer^g, M. Hussonnois^f, Y. Kadi^c, P. Karaiskos^j,
G. Kitis^l, R. Klapisch^c, P. Kokkas^k, V. Lacoste^a, C. Le Naour^f, C. Lópezⁱ, J.-M. Loiseaux^g,
J.M. Martínez-Valⁿ, O. Méplan^g, H. Nifenecker^g, J. Oropesa^c, I. Papadopoulos^l,
P. Pavlopoulos^k, E. Pérezⁱ, A. Pérez-Navarro^{m,(§)}, M. Perladoⁿ, A. Placci^c, M. Pozaⁱ, J.-P.
Revol^c, C. Rubbia^c, J.A. Rubio^c, L. Sakelliou^j, F. Saldaña^c, E. Savvidis^l, F. Schussler^g, C.
Sirventⁱ, J. Tamarit^b, D. Truber^f, A. Tzima^l, J. B. Viano^g, S. Vieiraⁱ, V. Vlachoudis^{a,l}, K.
Zioutas^l.

a) *CEN, Bordeaux-Gradignan, France*

c) *CERN, Geneva, Switzerland*

e) *Dip. di Fisica e INFN, Univ. di Padova, Italy*

g) *ISN, Grenoble, France*

i) *Universidad Autónoma de Madrid, Spain*

k) *University of Basel, Switzerland*

m) *Univer. Alfonso X el Sabio, Madrid, Spain*

b) *CEDEX, Madrid, Spain*

d) *CIEMAT, Madrid, Spain*

f) *IPN, Orsay, France*

h) *Sincrotrone Trieste, Italy*

j) *University of Athens, Greece*

l) *University of Thessaloniki, Greece*

n) *Universidad Politécnica de Madrid, Spain.*

(§) *Present address at LAESA, Zaragoza, Spain. Present address MIT, Cambridge, USA*

(†) *Present address CRS4, Cagliari, Sardegna, Italy*

Abstract

A short description of the set-up of the TARC experiment at CERN and the ARC principle is presented. This is followed by a very brief overview of the flux measurements and their comparison with the MC prediction. Then the method and specific set-up used for the integral transmutation of ^{99}Tc and ^{129}I measurements will be shown, indicating some of the actions taken to minimise systematic uncertainties. With this set-up the transmutation rate of ^{99}Tc and ^{129}I was measured in many positions around the lead block, corresponding to different neutron spectra and flux intensities. The experimental results and the excellent agreement with the MC predictions are discussed. Finally, the CeF_3 measurements of the energy dependence of the neutron capture on ^{99}Tc targets are explained. All these measurements confirm the ARC effect and its potentiality for LLFF transmutation.

Introduction

The TARC experiment conducted at CERN by an international collaboration including more than 14 institutions from different European countries and partially financed by the DGXII of the EU and some national agencies, is the second phase of the experimental program of the Energy Amplifier [1], EA. The objectives of the experiment can be grouped in two main lines: first, the measurement and simulation of the production of neutrons in large volumes of lead and their diffusion and moderation in this medium, and second, the measurement and simulation of the Transmutation by Adiabatic Resonance Crossing, ARC, of some of the most relevant long lived fission fragments, LLFF, mainly ^{99}Tc and ^{129}I .

The ARC principle is based on the lead properties. Lead is a material highly transparent to neutrons (very low absorption cross section from the MeV region down to very low energies) but with a moderate elastic neutron cross section that in addition is nearly energy independent in a large energy range (mean free path close to 3 cm) and with a high atomic mass that limits the maximum energy transfer in a neutron elastic collision (the minimum fraction of the original neutron energy after a collision is $\alpha \equiv ((A-1)/(A+1))^2 = 0.981$ for natural lead). Taking into account these properties it is easy to realise that if a neutron source, producing neutrons in the MeV region, is introduced in a large lead volume a high neutron flux will be developed with a neutron energy spectra nearly isoletargic. In other words neutrons produced at high energies will moderate very slowly their energy, moving over long distances without substantial change in their energies (high flux intensity) and, because of the low absorption, the total number of neutrons is conserved down to very low energies. The scattering cross section being constant provides in this way a nearly isoletargic flux, when integrated over the whole volume covered by the neutron flux. For any particular position this distribution is slightly modified depending on the spatial distribution of the neutron source.

The main element to achieve that high intensity flux is the very small energy loss per collision, for this reason we describe that process as *Adiabatic* neutron moderation. The isoletargic energy distribution of the flux allows to take full advantage of the resonances in the cross section of the transmutation process. In the case of LLFF, the transmutation takes place by neutron capture. For example when ^{99}Tc ($t_{1/2} = 2 \times 10^5$ y) captures a neutron produces ^{100}Tc that decays, with a half live of 15.8 s, to the stable ^{100}Ru . Several of the most offending LLFF in the nuclear wastes present important neutron capture resonances, Figure 1 for ^{99}Tc , making resonance capture in an adiabatic neutron flux, TARC, a promising method for the elimination of those wastes.

The verification of the TARC principle requires both the measurement of the neutron flux energy and space distribution and the experimental determination of the transmutation rates. In the following sections the experimental set-up, a brief description of the flux measurements techniques and results, the measurements of transmutation rates and their comparison with Monte Carlo simulations will be presented.

TARC experimental set-up

The main elements of the TARC experiment are a large lead block, the proton beam, and the DAQ system.

Figure 1 ^{99}Tc capture cross section

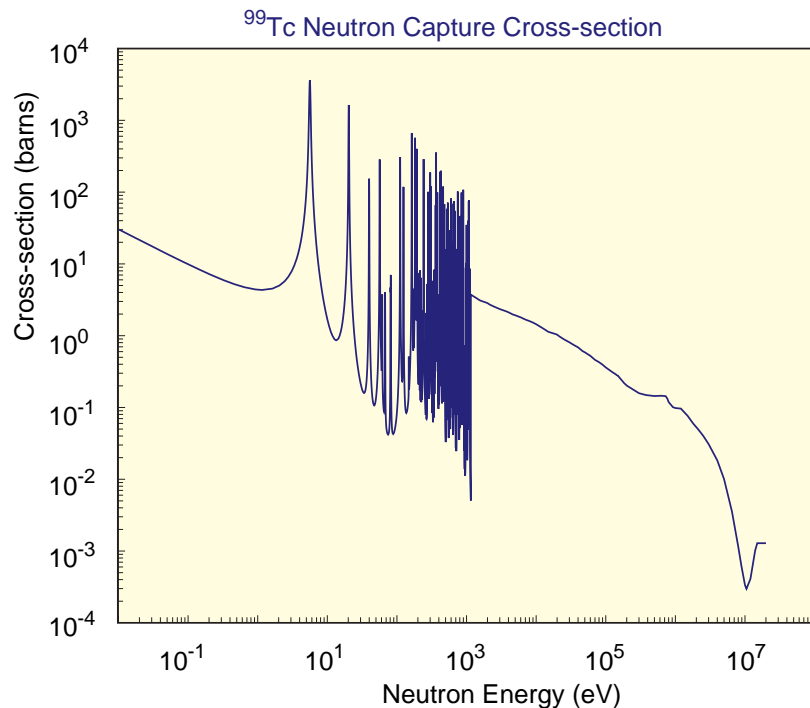


Figure 2 shows the arrangement of the 334 tons of pure lead where the neutrons, produced by spallation by the proton beam and diffused by the collisions with the lead nuclei make up the neutron flux. Lead has been commercially obtained with a nominal purity of 99.99%. This Lead purity has been exhaustively verified for nearly every element in the periodic table, by several techniques. The only relevant contaminations found were 19 ± 2 ppm of Bi and 3.6 ± 0.6 ppm of Ag. The block shape is close to a square parallelepiped, 3.3×3.3 m² of base and 3 m long, with the corners removed. It includes a 120 cm deep longitudinal beam hole, in the centre of the front face, and 12 full length longitudinal instrumentation holes.

A very flexible pulsed proton beam, extracted from the PS accelerator complex at CERN, has been used. The kinetic energies ranged from 200 MeV to 2.75 GeV, and the beam intensities varied from 10^3 to 10^{10} protons per shot. The beam intensity has been measured, shot by shot, by two systems. The first one, for high intensities, was based on a pair of beam transformers, Figure 3, which provided an intrinsic resolution of 1%. The absolute calibration was based on the irradiation of Al foils. A global uncertainty of 5% was achieved on the beam intensity determination. The beam instrumentation included also multiwire proportional chambers, MWPC, that measured the position and angle of the beam. For very small beam intensities a scintillators hodoscope allowed to count the actual number of particles arriving to the lead beam hole at each shot.

The advanced DAQ system was based on VME and CAMAC modules, recorded more than 200 Gbytes of data and allowed the on-line monitoring of the data quality.

Figure 2 TARC lead block, transverse view

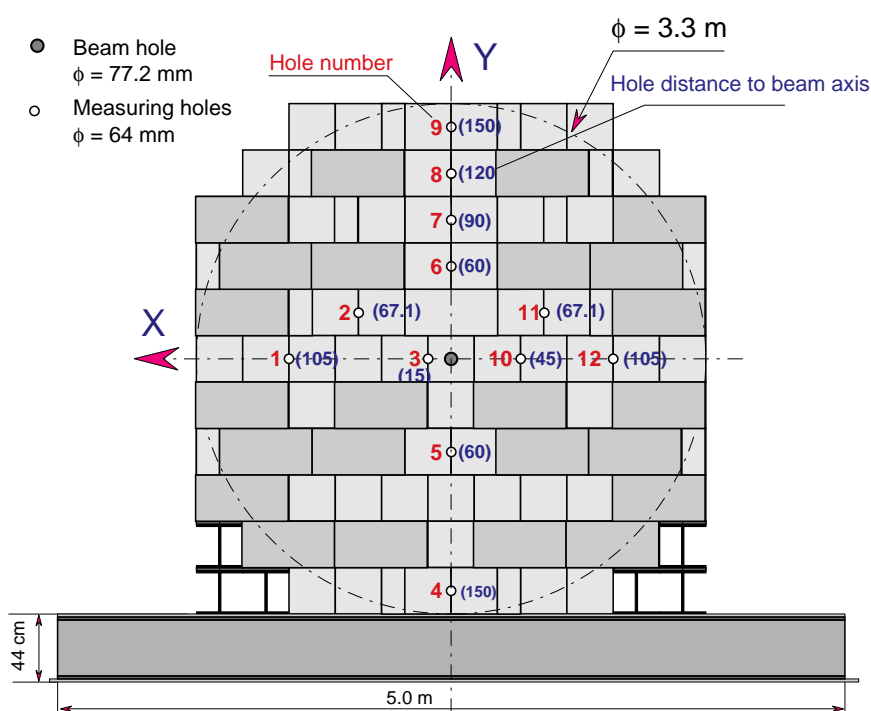
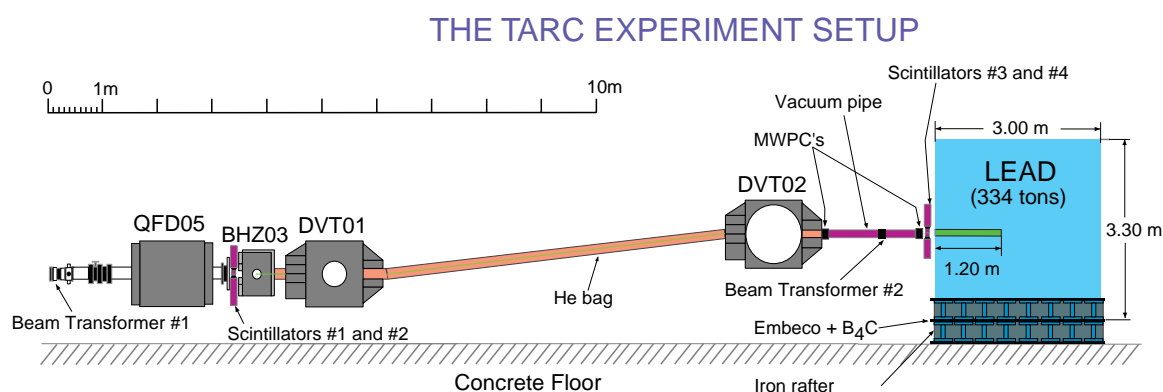


Figure 3 Longitudinal view of the beam instrumentation close to the experimental area

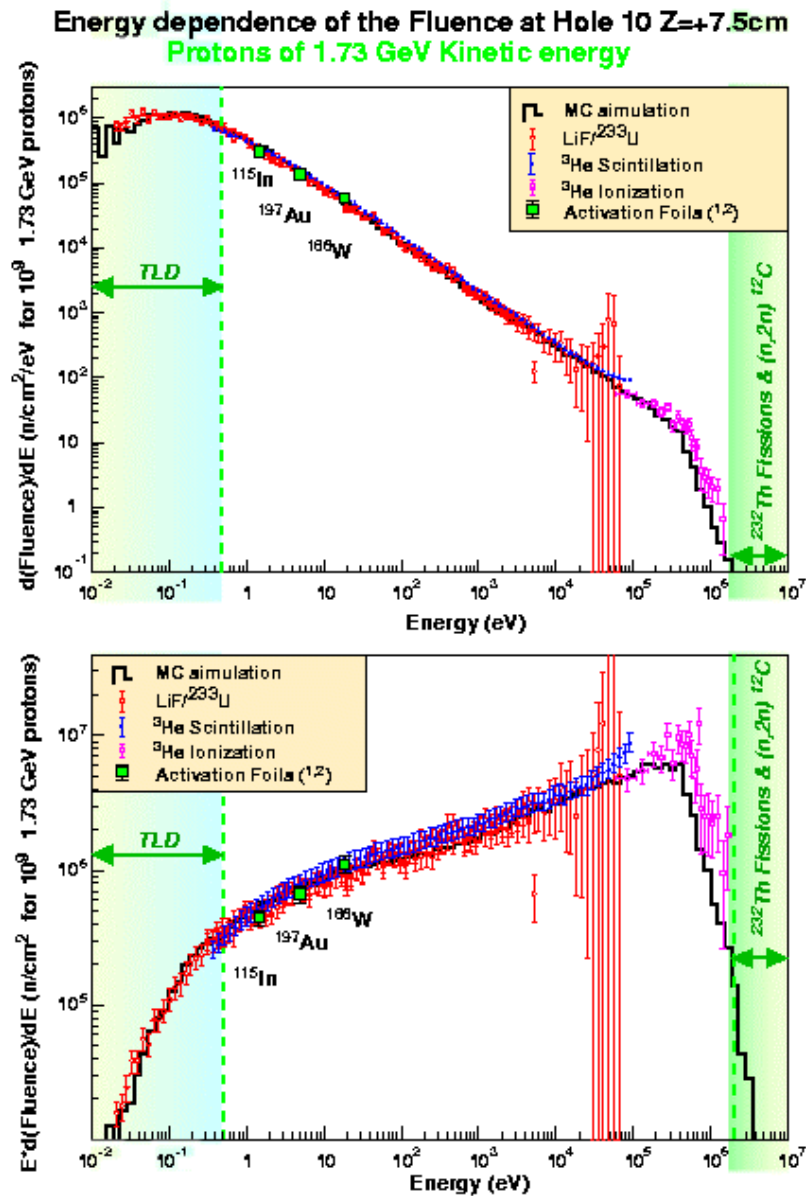


Neutron flux measurements

A large panoply of neutron detectors, including ^3He (ionisation and scintillation), $^6\text{Li} + \text{Si}$ detectors, Activation foils, Thermoluminescence detectors and Track etching detectors, placed in successive measurements at different positions inside the instrumentation holes, has provided a very detailed map of the neutron flux for the full neutron energy range, from thermal energies to few MeV. The details of the different detectors can be found somewhere else [2,3,4,5]. From the point of view of the LLFF transmutation experiments, the most relevant energy region, 0.1 eV to 1000 eV, is covered by the ^3He scintillation detector and the (^6Li , ^{233}U) + Si counters. Both detectors rely on the time to energy relation, characteristic of the neutrons moving in a slowing down lead spectrometer [6] to compute the energy of the detected neutrons. This relation has been calibrated in TARC with the help of a CeF_3 scintillator and samples with known resonances. As an additional verification, the neutron fluence has been measured at precise energies in a completely independent way, using activation foils. Foils of ^{115}In (1.457 eV), ^{107}Au (4.9 eV) and ^{186}W (18.8 eV) have been used in TARC.

Figure 4 shows the measurements, from all detectors, of the neutron fluence, as a function of the neutron energy, at the instrumentation hole #10 and at co-ordinate Z=+7.5 cm, for a proton kinetic energy of 1.73 GeV. The detector redundancy together with the repetition of measurements at symmetrical positions and different beam energies, and the excellent agreement of measurements from different detectors have provided a very strict control of systematic uncertainties.

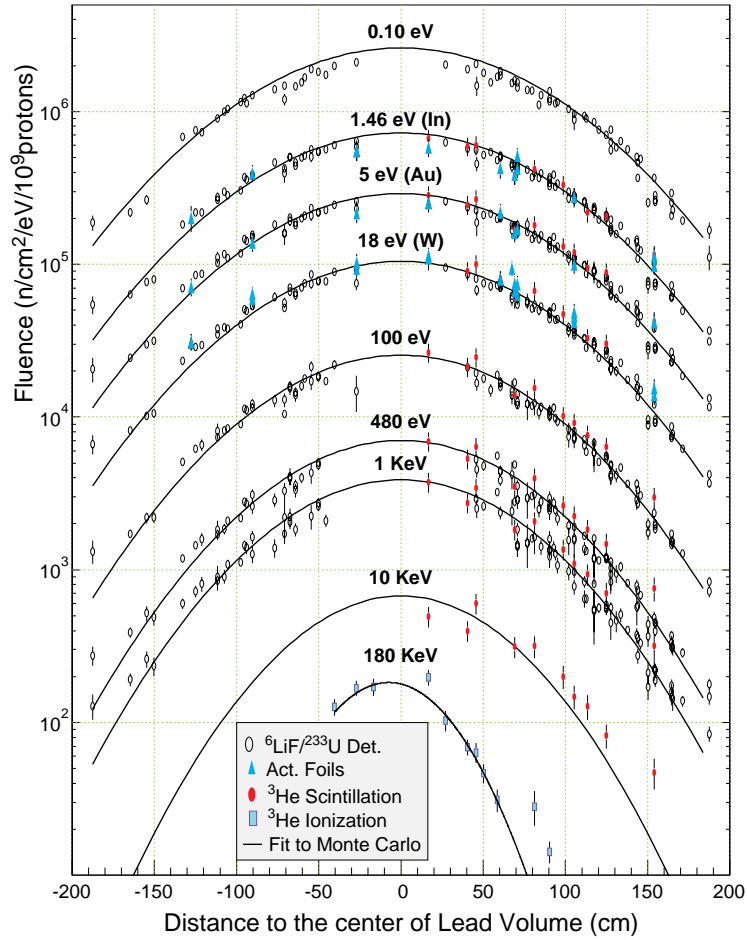
Figure 4 Neutron fluence neutron energy spectra measured at TARC



Notes: 1) Data scaled from 2.75 GeV kinetic energy. 2) Data scaled from different (close) position.

Many measurements were made with those detectors at different positions. Maps of the fluence at different energies have been built from these measurements. Figure 5 shows the space distribution of the fluence, for energies from 0.1 eV to 180 KeV, for a proton kinetic energy of 2.75 GeV, versus the distance to the lead block centre multiplied by the sign of the Z co-ordinate. Even when a perfect spherical symmetry is not expected, the data can be approximately described by a simple gaussian function of this distance, as expected from the Fermi age theory for a punctual source in an infinite lead volume.

Figure 5 Experimental spatial distribution of the neutron fluence for different energies



Both figures show the excellent agreement of the Monte Carlo predictions, for all the positions and energies, with differences to the data of the order of 10 to 15%, in the energy range most relevant to ARC.

Transmutation of ^{99}Tc

In the TARC experiment the ^{99}Tc transmutation was directly measured for macroscopic samples (close to 1 gram) in different conditions both of the sample and of the neutron flux energy spectra and intensity. In addition to the interest of the direct data by themselves, they allow to verify the available evaluated cross sections and the simulation tools. The ability to study situations with largely different contributions of the resonance region to the ^{99}Tc transmutation and the study of situations with large selfshielding effects was especially interesting.

Figure 6, shows a simplified scheme of the ^{99}Tc transmutation process. ^{99}Tc , already radioactive with a half live of 2.111×10^5 years, after capturing a neutron becomes ^{100}Tc , usually in an excited state. This state decays very fast (typically in few ns) into ^{100}Tc ground state, by emitting the so-called *prompt* photons. At a much slower rate, half-live of 15.8 s, ^{100}Tc decays by a β^- transition to ^{100}Ru , about 7% of the cases into excited states of this isotope. Then, these ^{100}Ru excited states decay very fast, in less than 1 ns, into the ^{100}Ru ground state, emitting the so-called *delayed* photons.

The absolute transmutation rate is determined at TARC from the measured rate of these delayed photons. The measurement is integral in the sense that it includes the contribution

from the transmutation produced by neutrons of all the energies. Because of the uncertainty on the fraction of ^{100}Tc decays including one or more photons, our measurement of the transmutation rate has a systematic error of 14%. This has become the dominant component of the TARC measurement of the ^{99}Tc transmutation rate. However special care has been applied to keep all the other systematic errors at their minimum level, in such a way that, whenever more precise information on the ^{100}Tc decay is available, the TARC data resolution can be improved.

Figure 6 Simplified scheme of the ^{99}Tc transmutation process

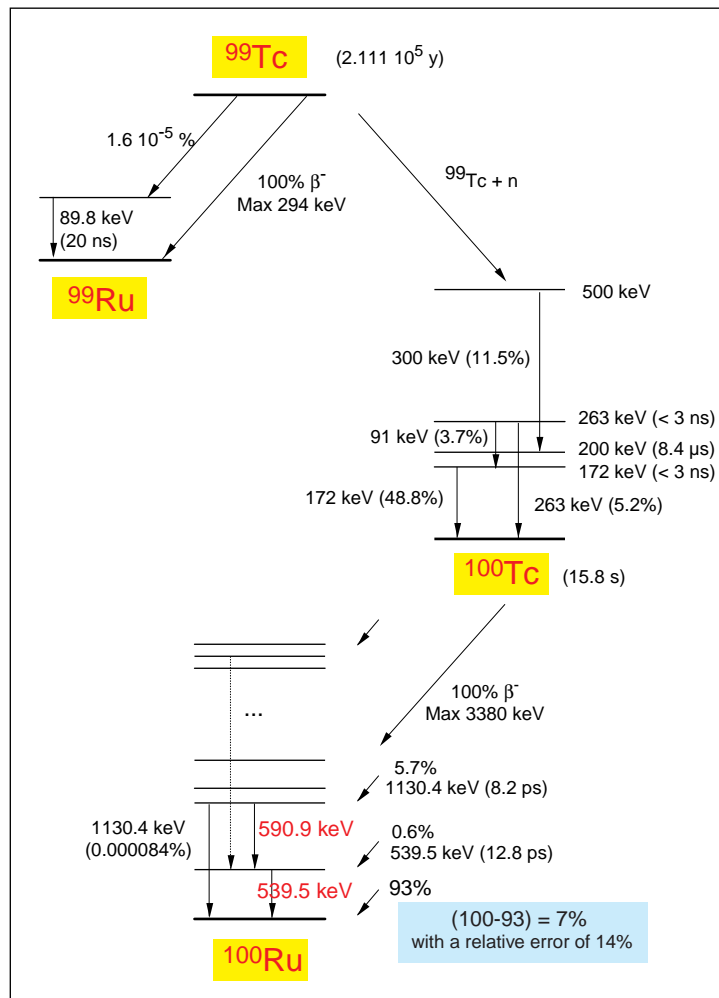
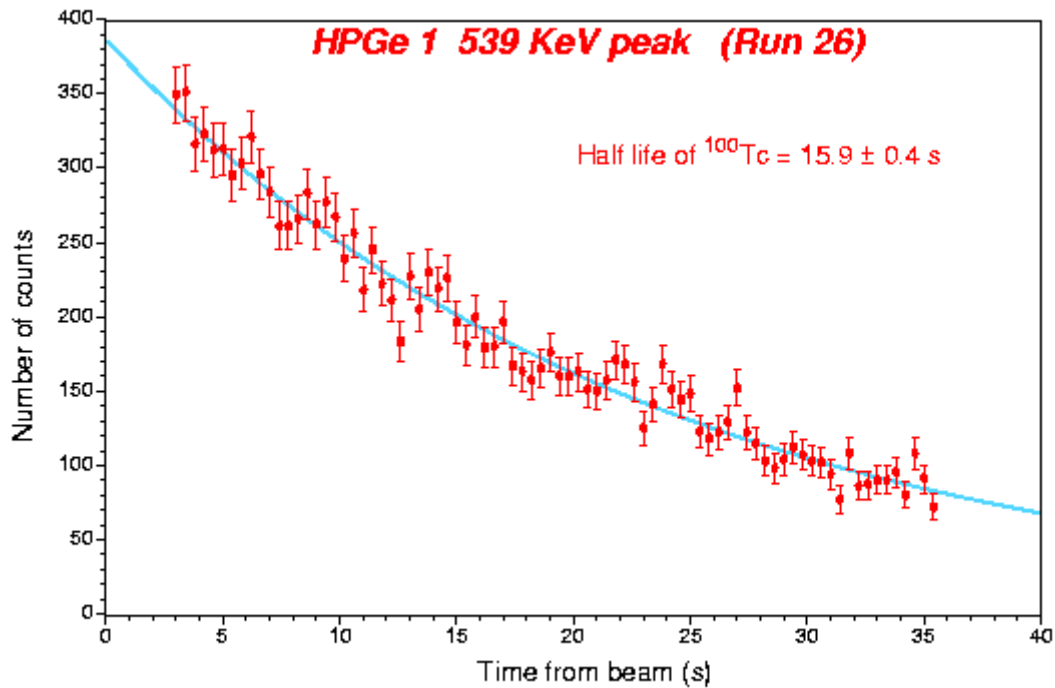


Figure 7 Experimental determination of the ^{99}Tc half-live



The short half live of ^{100}Tc , verified at TARC in a special experiment, Figure 7, makes difficult the accumulation of the large statistics required to achieve the 1% statistical precision of TARC. This difficulty is overcome by using a pneumatic system, called *Rabbit* and described schematically at Figure 8, that transfer cyclically the sample between the irradiation position and the measuring station after each pulse of the CERN-PS proton accelerator. In this way and with a precise measurement of the beam intensity, pulse by pulse, it was possible to accumulate as much statistic as required with modest mass samples and neutron flux intensities. This figure also shows the shape of the container and sample used in most of the ^{99}Tc transmutation experiments, that consist on 441 mg of KTcO_4 powder.

Figure 8 Scheme of the TARC Rabbit system

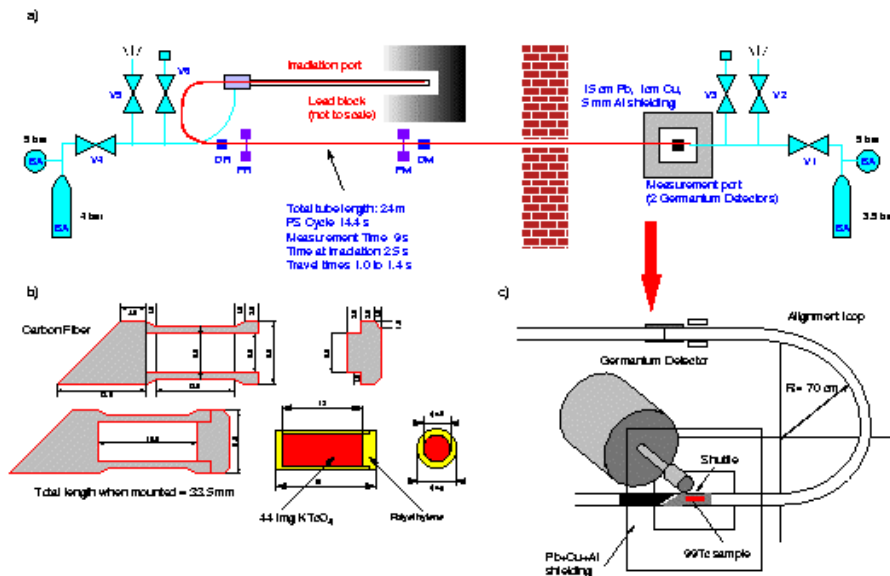


Figure 9 shows a transverse view of the *Rabbit* measuring station. All the elements of this station have been carefully set-up to reduce the instrumental systematic errors. This includes a very large detector shielding with more than 15 cm of lead and the use of redundant instrumentation by installing two large independent HPGe counters. In addition detailed studies and appropriated correction had been applied for every single aspect of the experiment, including: the samples masses, the calibration of the HPGe detectors, the photon absorption in the sample itself and in the transport capsule, the beam intensity and quality, the position of the sample during the measurement at each *Rabbit* cycle, the accidental and correlated pileups, the system dead time, the electronic failures and the procedure for evaluation of the number of signals inside each photon line. As a result of these efforts we estimate in 8% the total instrumental systematic error of the ^{99}Tc transmutation rate measurement at TARC.

Figure 9 Transverse view of the *Rabbit* measuring station

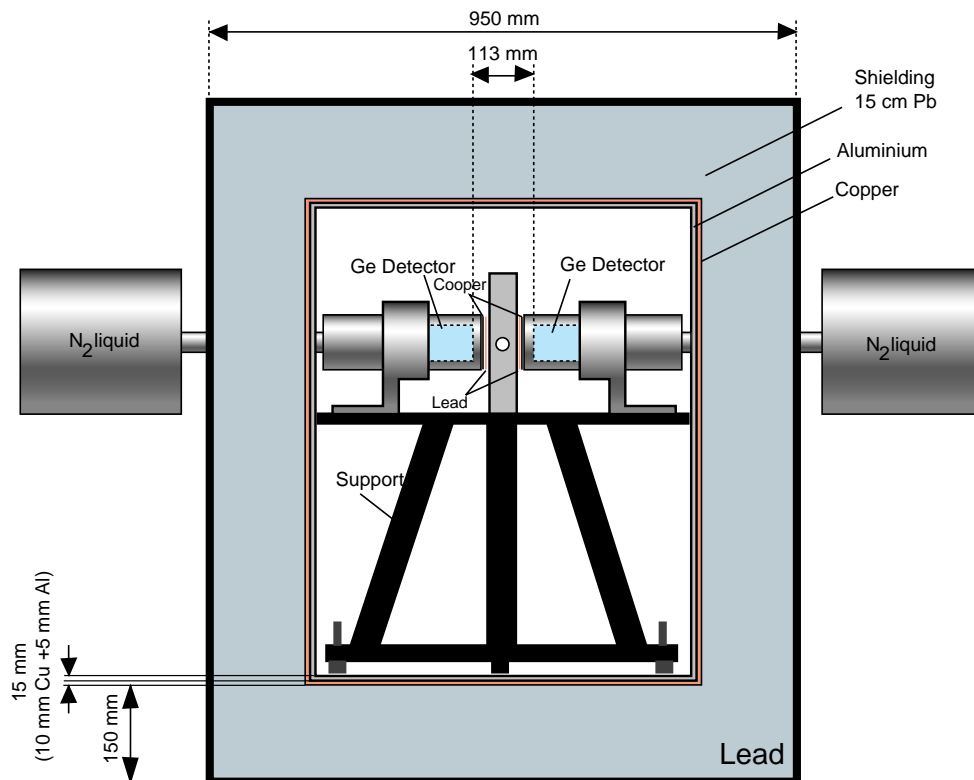


Figure 10 shows the spectrum of photons collected by one of the HPGe counters from the sample during one set of irradiations. The spectrum shows the characteristic set of lines corresponding to the decay of ^{100}Tc into the excited states of ^{100}Ru . Two prominent lines can be found at 539 KeV and at 590 KeV. The resolution of the HPGe counter at these energies is of 2-3 KeV and even when the background is very small, note that the vertical scale in Figure 10 is logarithmic and that the detail in the corner shows the 539 peak in linear scale, this background has been carefully discounted from the activity on the line. Both photon lines had been used independently to compute the transmutation rates, and combining this fact with the use of two detectors, a four-fold redundancy in the ^{99}Tc transmutation rate determination was available at TARC. This redundancy has provided an exceptional control of the possible instrumental systematic effects. In the Figure there are a few lines produced from the impurities in the sample, ^{137}Cs and ^{98}Tc , the intensity of these peaks is independent of the irradiation and this fact has also been used to control the data quality.

Figure 10 Spectrum of delayed photons from the ^{99}Tc sample after irradiation

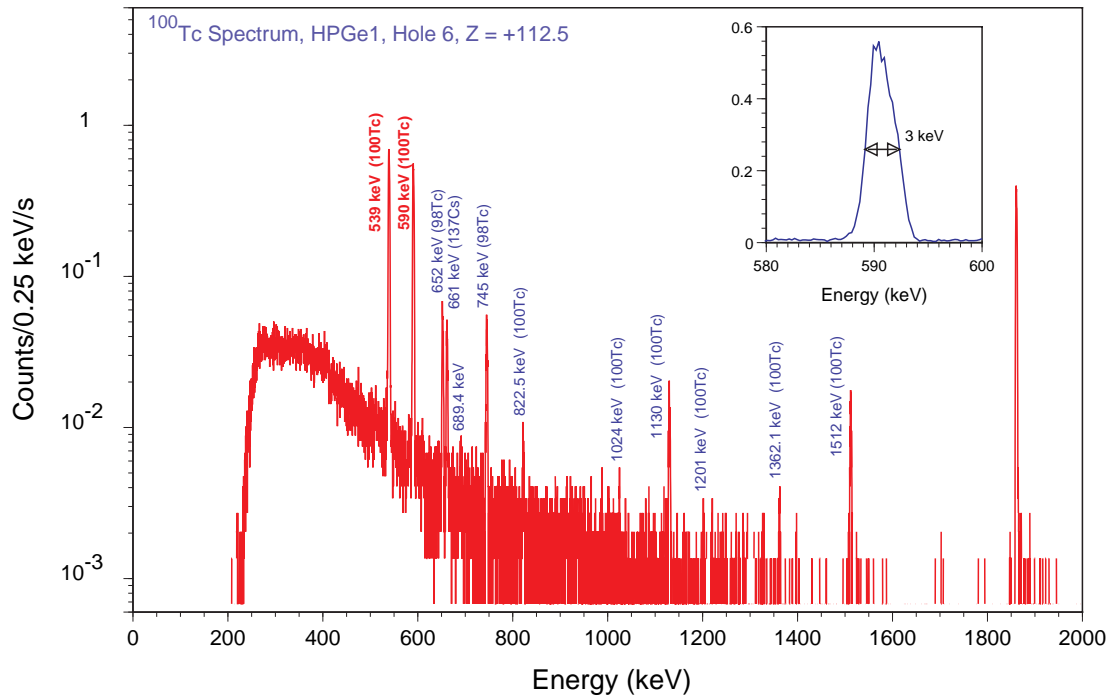
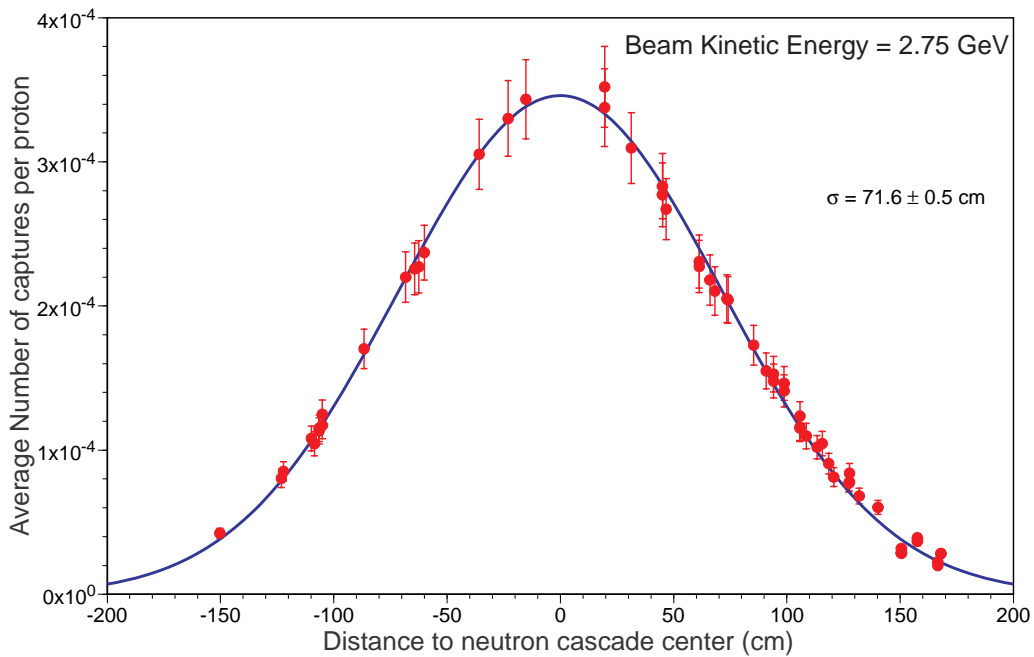


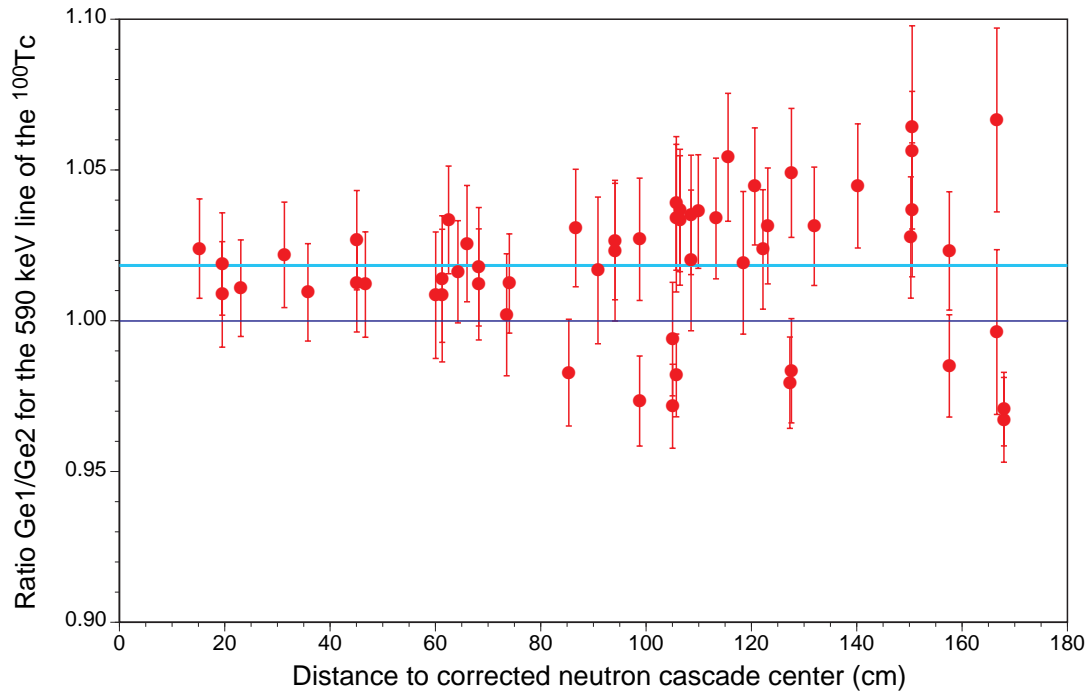
Figure 11 ^{99}Tc transmutation rate, for a sample with 216.1 mg of ^{99}Tc and for 2.75 GeV kinetic energy protons, as a function of the irradiation position in the TARC lead block



With this system and careful analysis, a large set of measurements had been performed irradiating the sample at more than 50 positions distributed all around the TARC lead block. Figure 11 shows the average number of captures in ^{99}Tc , or ^{99}Tc transmutations, per proton in the different positions, as a function of the distance to the neutron cascade centre times the sign of the Z co-ordinate. The transmutation rate for a sample with 216.1 mg of ^{99}Tc , placed at 45 cm from the lead block centre, is 2.67×10^{-4} transmutation per 2.75 GeV proton and the total error is 16%. The different data are very coherent one to each other, show a high degree of isotropy (except for the farthest points that are too close to the lead block surface) and can

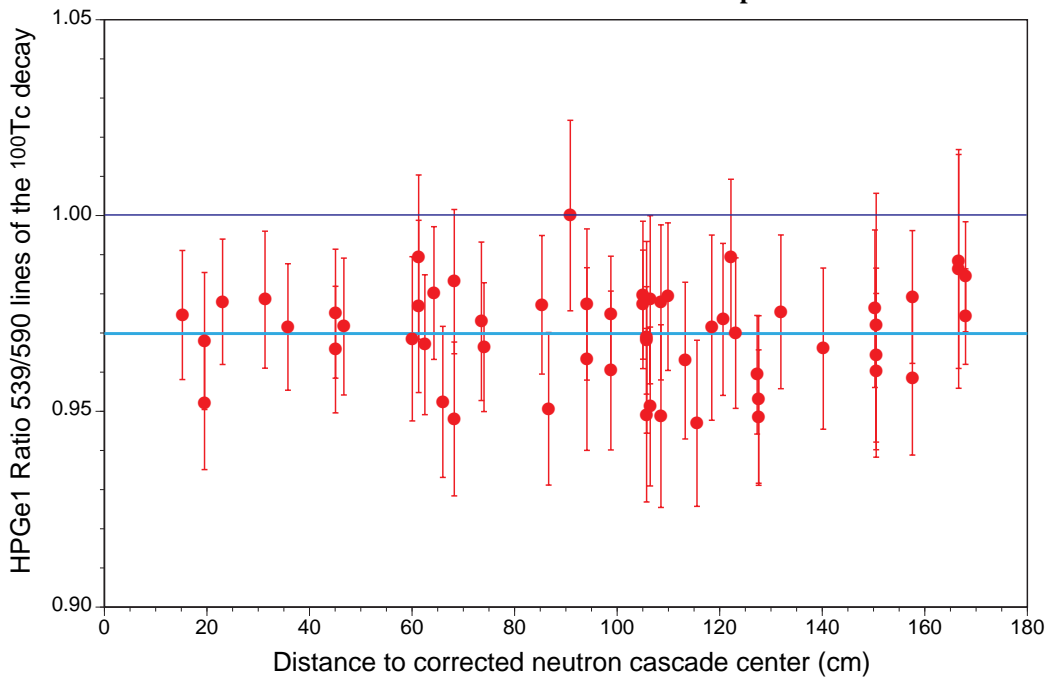
be approximately described by a gaussian function with parameters very close to those corresponding to the neutron flux distribution in the range from 1 to 100 eV. This behaviour is expected from the large contribution of the two main capture resonances (5.9 and 20 eV) to the ^{99}Tc transmutation in the TARC experimental conditions.

Figure 12 **Ratio of the transmutation rates measured by the two different HPGe counters from the 590 KeV photon line as a function of the irradiation position**



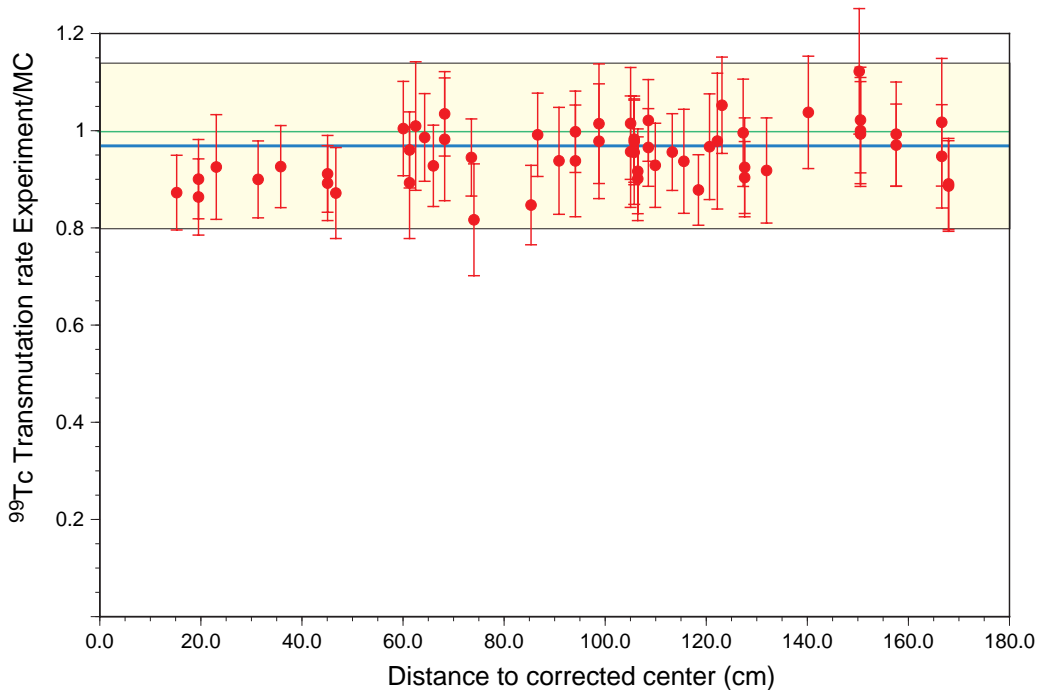
A verification of the low level of systematic errors is provided by the Figures 12 and 13. The first figure shows the ratio of transmutation rates obtained from the data of the two different HPGe counters from the same ^{100}Tc photon line (590 KeV). This figure is sensible to the systematic errors on the efficiency and dead time of the counters, and all the points are compatible within errors with a constant ratio corresponding to 2% systematic error. On the other hand, Figure 13 shows the ratio of the estimated ^{99}Tc transmutation rates by using the two photon lines for the same HPGe counter as a function of the irradiation position. This figure, that will show systematic errors on the angular correlation corrections, photon absorption in the instrument materials, peak reconstruction and relative probability of the two lines, is also compatible within errors with a constant value corresponding to a systematic error of 3%.

Figure 13 **Ratio of the transmutation rates measured by using the two photon lines for the same HPGe counter as a function of the irradiation position**



Previous graphs have shown the quality of the data, Figure 14 shows the comparison of the experimental data with the predictions of a complete Monte Carlo simulation of the ^{99}Tc transmutation process at the TARC experiment, using the Energy Amplifier simulation system [7,8,9] and the JENDL 3.2 nuclear data libraries. An excellent agreement is found for all the positions, with an average deviation smaller than 5% well below the 14% uncertainty on the fraction of ^{100}Tc decays with photons. All the points are consistent with this deviation within the errors bars displayed in the figure that include only the statistical and instrumental systematic uncertainties.

Figure 14 **Ratio Data/Monte Carlo for the ^{99}Tc transmutation rate as a function of the irradiation position**

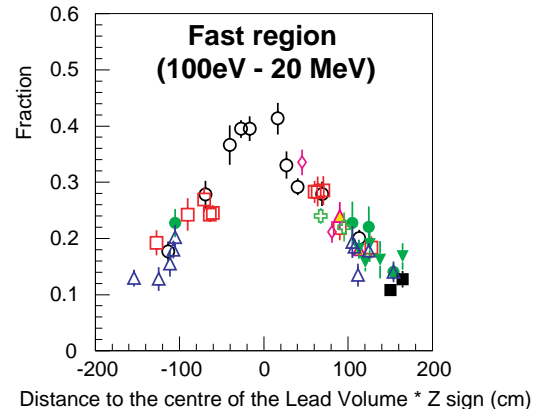
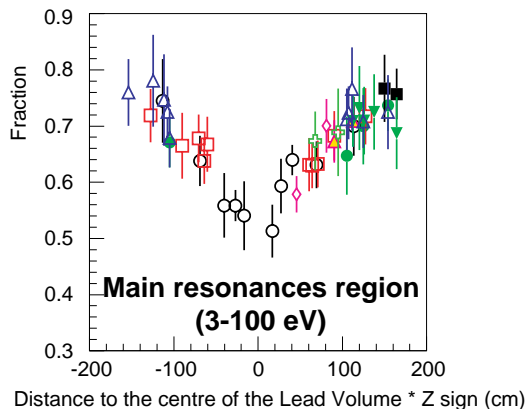
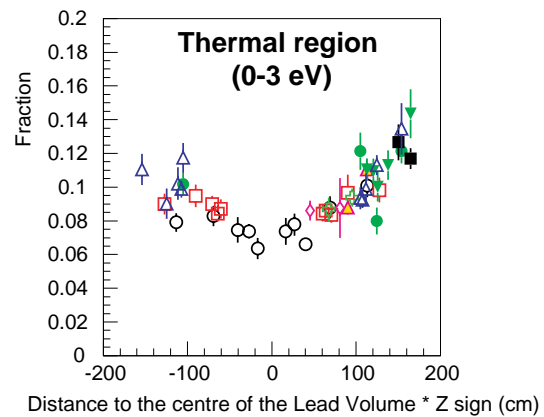


The complexity of the simulation and the relevance of the agreement are clarified by Figures 15 and 16. Figure 15 shows the fraction of ^{99}Tc transmutation produced by neutrons of different energy ranges: thermal region (0-3 eV), the main resonances region (3-100 eV) and the fast region (100 eV-20 MeV) as a function of the irradiation position, according to the Monte Carlo simulation. These graphs show the substantial change in the contributions from resonance and fast neutrons to the ^{99}Tc transmutation, from the centre to the periphery of the lead block, as a consequence of the neutron energy spectrum evolution with the position inside the lead block.

Figure 15 Monte Carlo estimated contributions from the different neutron energy ranges as a function of the irradiation position

Fraction of captures in ^{99}Tc for different energy ranges from MC simulations

- Hole 1: X= 105 Y=0 cm
- Hole 3: X= 15 Y= 0 cm
- Hole 4: X= 0 Y= -150 cm
- Hole 6: X= 0 Y= 60 cm
- ▲ Hole 7: X= 0 Y= 90 cm
- ▼ Hole 8: X= 0 Y= 120 cm
- ◇ Hole 10: X= -45 Y= 0 cm
- ⊕ Hole 11: X= -60 Y= 30 cm
- △ Hole 12: X= -105 Y= 0 cm



On the other hand, Figure 16 shows the experimental data of the transmutation rates, at a fixed irradiation position, for three different samples of ^{99}Tc . The samples have different masses, density and chemical form (2 samples are KTcO_4 and one is a very thin Tc metallic foil). The data show that shelfshielding levels as high as 50% are suffered by the heavier sample. The figure also presents the Monte Carlo simulation, in excellent agreement with the data. Shelfshielding is a function of the neutron spectra and consequently of the irradiation position, changing the magnitude from point to point in Figure 14, the agreement at all the position shows a correct description of the effect by the Monte Carlo with the JENDL 3.2 database. Further details on the integral measurements of the ^{99}Tc transmutation can be found at [10,8,9].

Figure 16 Experimental data and Monte Carlo predictions for the ^{99}Tc transmutation rate, normalised to the sample mass, for three different samples with different masses and chemical compositions

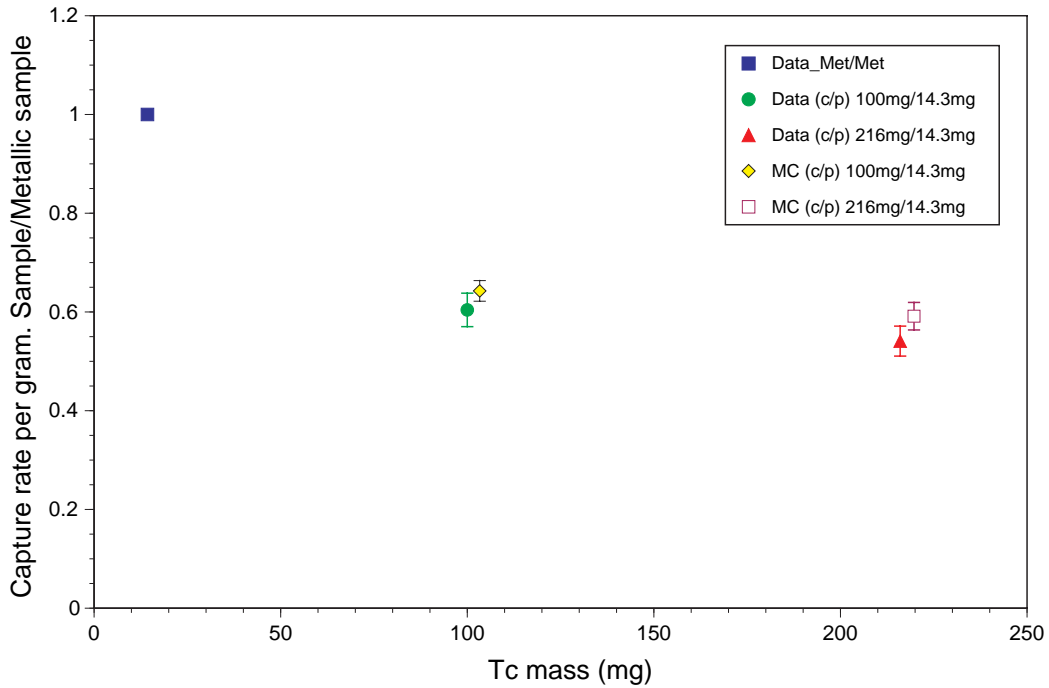
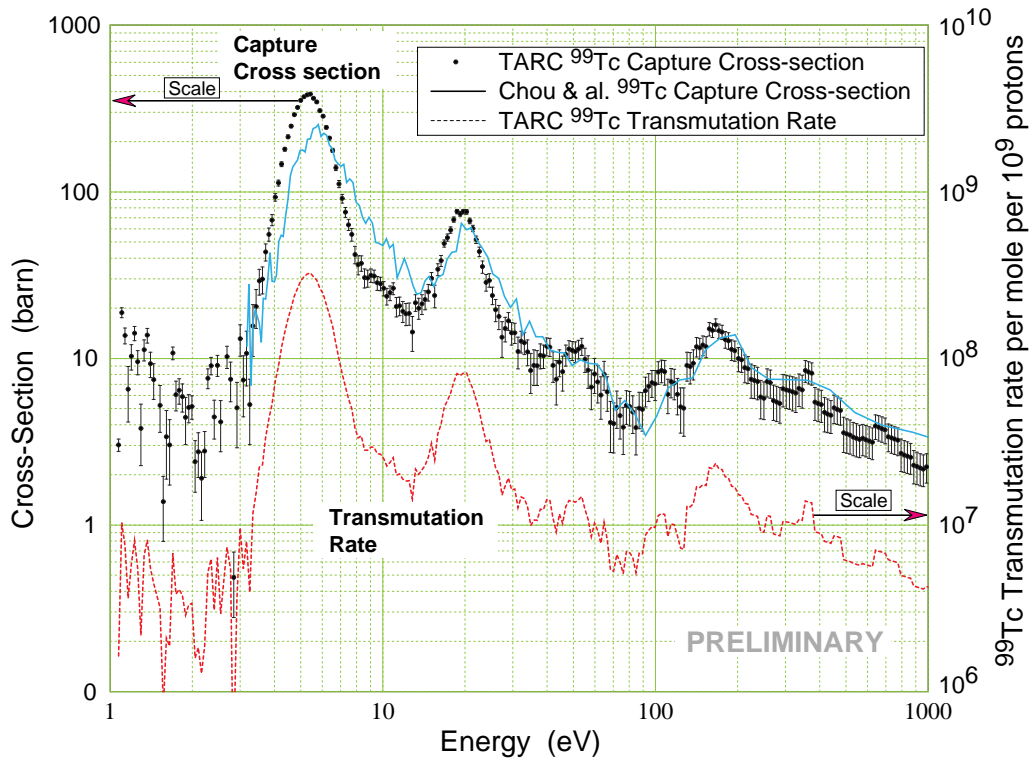


Figure 17 ^{99}Tc transmutation rate as a function of the neutron energy and ^{99}Tc apparent neutron capture cross section



In addition to the integral measurements, the dependence of the transmutation rate with the neutron energy was measured from the prompt photons emitted after the neutron capture, with the help of a CeF_3 scintillator and using the characteristic relation between detection time

and neutron energy of lead slowing down spectrometers, already mentioned. Figure 17 show this dependence for a ^{99}Tc sample irradiation position at 45 cm from the lead centre and a proton kinetic energy of 2.75 GeV. The apparent neutron capture cross section of ^{99}Tc , obtained from this curve and the neutron flux energy spectra experimentally measured, is also shown in the figure in comparison with the previous Chou et al measurements [11]. Much better statistics and resolutions had been obtained at TARC. This apparent capture cross section is an additional element for cross checking the available nuclear data libraries. Further details on the integral measurements of the ^{99}Tc transmutation can be found at [8,9].

Transmutation of ^{129}I

The ^{129}I fission fragment with a half live of $1.57 \times 10^7 \text{y}$, is together with ^{99}Tc , one of the most offending isotopes in the nuclear wastes at very long times. The measurement technique used for iodine is simpler than for technetium because the half-lives of the resulting isotopes are long enough and no *Rabbit* was required. On the other hand the analysis is more difficult. Figure 18 shows the scheme of nuclear reactions taking place in the sample during the ^{129}I transmutation. When ^{129}I captures a neutron produces ^{130}I excited states, but as ^{130}I has two isomers, a fraction of the reactions will decay immediately to the ground state but another part will populate the $^{130\text{m}}\text{I}$ isomer. Then the $^{130\text{m}}\text{I}$ can either decay to the ground state or directly decay to ^{130}Xe . Finally, the ^{130}I ground state nuclei will also decay to ^{130}Xe . The delayed photons produced in the last 3 decays have been used at TARC to evaluate the transmutation rate of the sample.

Figure 18 Scheme of nuclear reactions taking place in the TARC ^{129}I sample during its transmutation

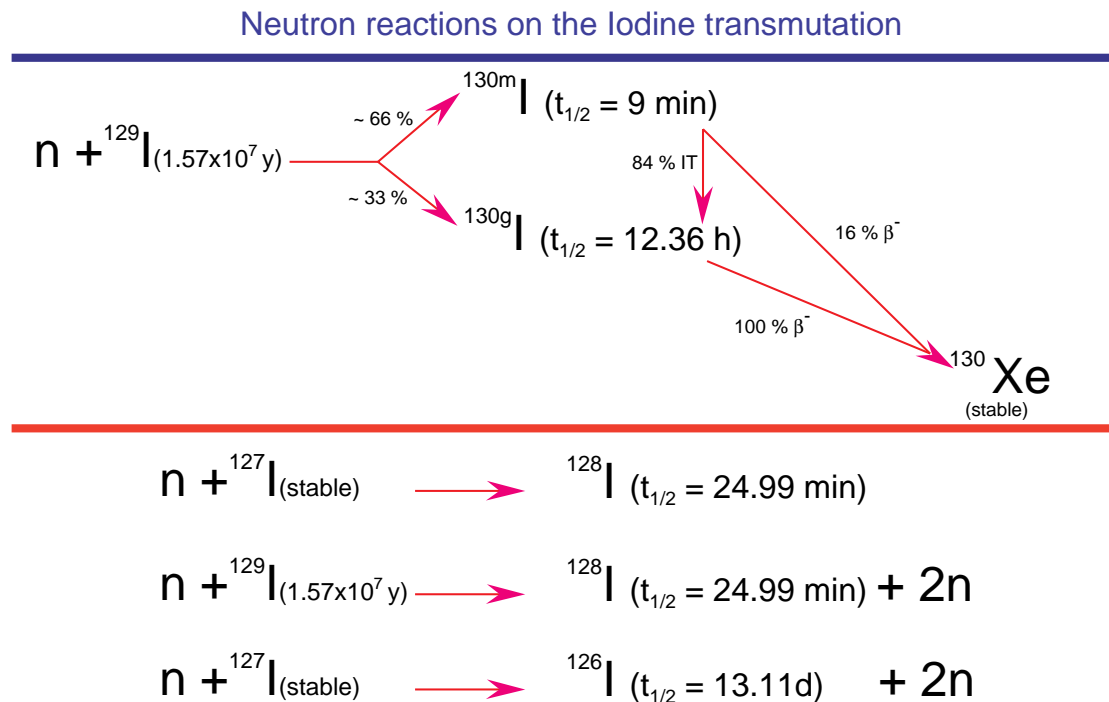


Figure 19 Geometry and characteristics of the ^{129}I sample used at TARC

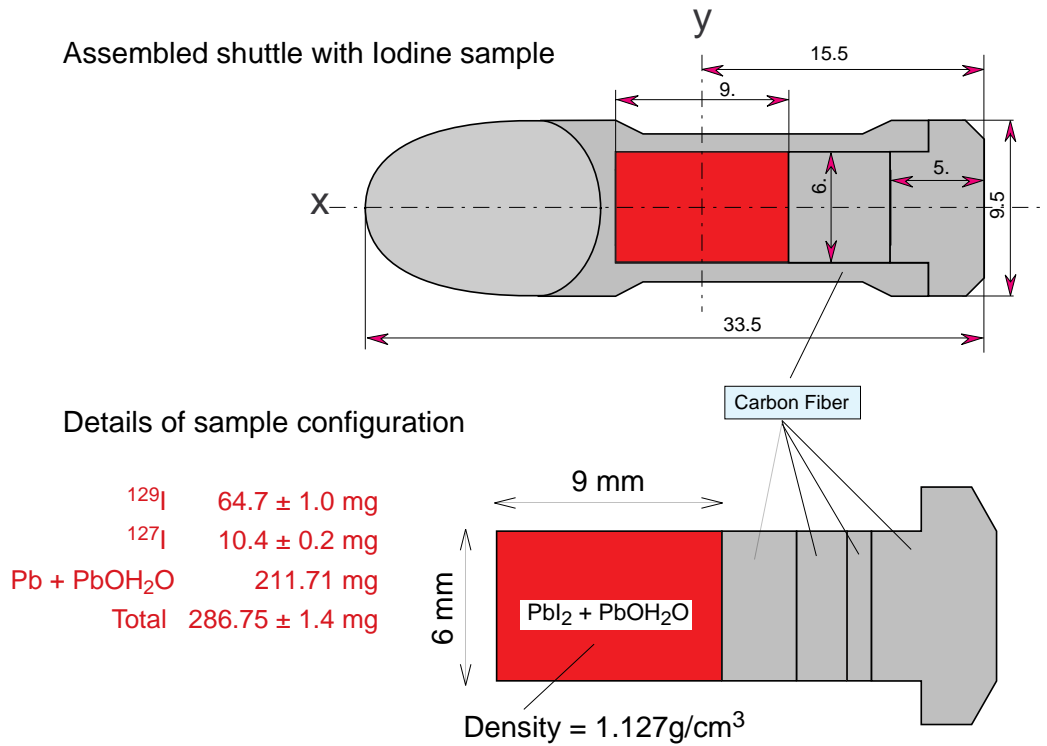
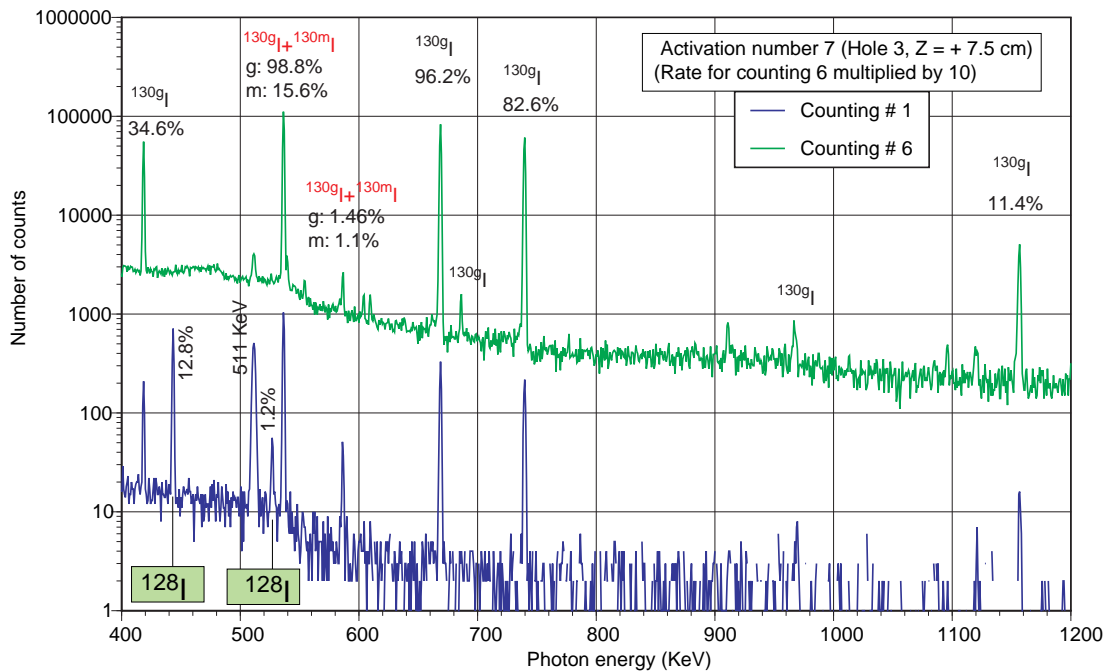


Figure 20 Photon spectra collected from the ^{129}I sample at two different times after irradiation



In addition to ^{129}I , the sample whose geometry and characteristics are shown at Figure 19, contains the stable isotope ^{127}I and, in consequence, ^{128}I is also produced during the irradiation. Figure 20, shows two photon spectra obtained from the PbI_2 sample after irradiation. The bottom one, correspond to a short counting taken shortly after irradiation and include the contribution from the $^{130\text{m}}\text{I}$ ($t_{1/2} = 9 \text{ min}$). In the upper spectra, taken several hours later, the contribution from $^{130\text{m}}\text{I}$ is negligible and all the peaks are only populated by $^{130\text{g}}\text{I}$, with a half-life of 12.36 h. Using several counting measurements at different times after

irradiation it was possible to compute the production probability of each isomer of the ^{130}I in the neutron capture by ^{129}I . There is very little experimental information on this parameter and certainly no previous data for the TARC neutron spectra.

Figure 21 **Ratio of $^{130\text{m}}\text{I}/^{130\text{g}}\text{I}$ production in the ^{129}I transmutation measured at TARC (a) and comparison with previous values of this parameter (b)**

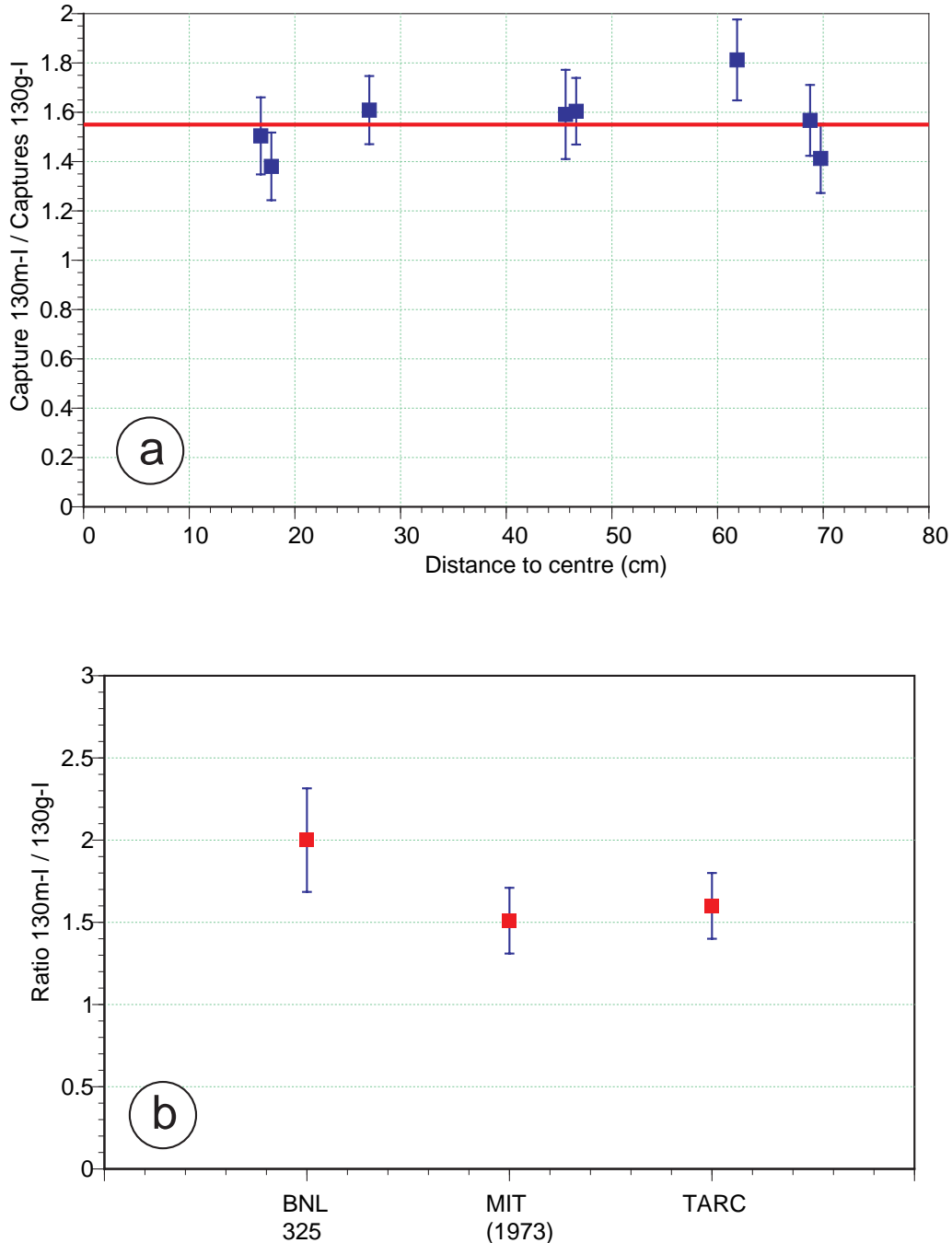
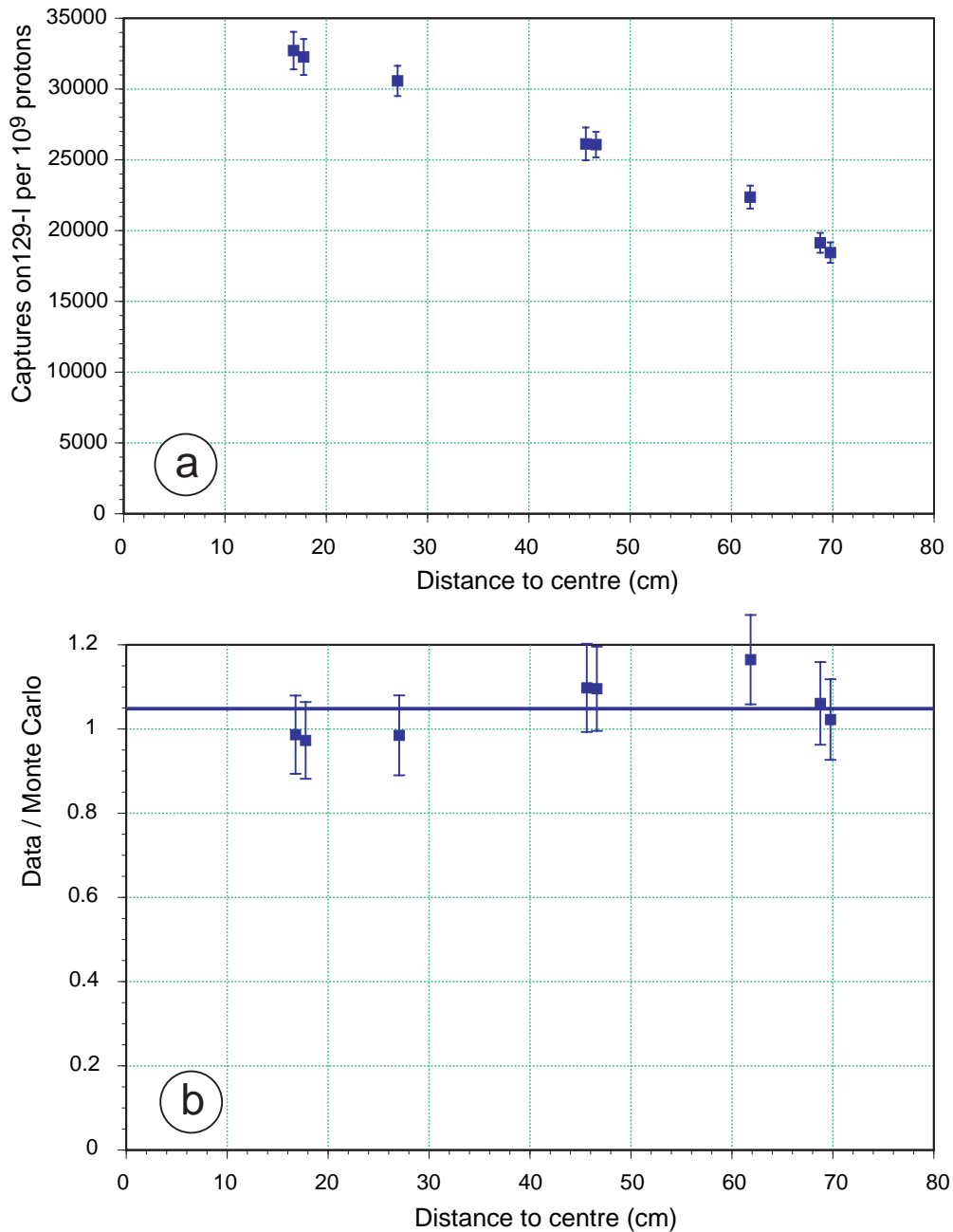


Figure 21a shows the values obtained for this parameter in irradiations performed at different positions inside the lead block. All the data is consistent with a constant value of $^{130\text{m}}\text{I}/^{130\text{g}}\text{I} = 1.55$, that, as can be seen at Figure 21b, is in good agreement with the only 2 previous data available, to our knowledge, from MIT [12] and BNL [13].

Using this value of the isomers production ratio, it was possible to compute the absolute ^{129}I transmutation rate. Figure 22a shows the dependence of this transmutation rate with the position of the sample for a kinetic energy of the protons in the beam of 2.75 GeV. The shape

of this curve is similar to the one obtained for ^{99}Tc , the systematic error 10% is also similar, but the absolute transmutation rate value is 2.5×10^{-5} per 2.75 GeV proton, for a sample with 64.7 mg of ^{129}I placed at 45 cm from the lead block centre, is smaller than for the ^{99}Tc , taking into account the different masses of the samples. Finally, Figure 22b presents the ratio between the measured data and the Monte Carlo simulations. As in the ^{99}Tc case, an excellent agreement is found validating both the simulation program and the used nuclear data libraries. Further details on the ^{129}I transmutation measurements can be found at [14,8,9].

Figure 22 ^{129}I transmutation rate, for a sample with 64.7 mg of ^{129}I and protons with 2.75 GeV kinetic energy, as a function of the irradiation position (a), and ratio data/Monte Carlo (b)



Conclusions

The TARC experiment has performed a comprehensive set of measurements for the characterisation of the neutronics in lead and of the adiabatic resonance crossing method for transmutation of long lived isotopes. In this last respect, a large set of direct measurements of the transmutation rates of ^{99}Tc and ^{129}I has been obtained at different irradiation positions inside the TARC lead block, corresponding to different neutron flux energy spectra. These spectra are similar to the ones foreseen for the EA reflector zone where the transmutation of those isotopes could take place. The special efforts on the setting up and analysis of the experiment has allowed to achieve a complete control of systematic effects and absolute resolutions close to 15%.

The TARC experiment do not correspond to the optimum situation for transmutation of these isotopes, however it has demonstrated the adiabatic resonance crossing principle, whose corollary is that the neutron cross section resonances can be used to improve the transmutation efficiency for these isotopes. In addition, because of the excellent agreement between the experimental data and the simulation, the TARC experiment has validated both the Monte Carlo program and the nuclear data libraries used to simulate the experiment, within the experimental resolution. These validated tools can be used to design specially optimised transmutation devices, either for specific isotopes or for isotope families, taking into account all the requirements of each installation.

Acknowledgements

The enthusiastic and professional support from CERN, in particular from the PS and TIS Divisions and the ECP group, that made possible the experiment are greatly appreciated. We would like to thank the DGXII of the European Union for their financial support, and to express our acknowledgement to the other funding institutions: Centre National de Recherche Scientifique and IN2P3 in France and Empresa Nacional de Residuos Radioactivos S.A., Comisión Interministerial de Ciencia y Tecnología and the Agrupación Eléctrica para el desarrollo de la Tecnología Nuclear in Spain.

REFERENCES

- [1] Rubbia *et al.*, *Conceptual design of a fast neutron operated high power energy amplifier*. CERN/AT/95-44 (ET), (1995).
- [2] Gonzalez *et al.*, Update of the TARC experiment results. Presented at the *Technical Committee Meeting on Feasibility and Motivation for Hybrid Concepts for Nuclear Energy Generation and Transmutation* organised by IAEA at CIEMAT. Madrid, 1997.
- [3] P. Pavlopoulos *et al.*, *Low Energy flux Measurements (at TARC)*. Workshop on P&T strategy studies and transmutation experiments. Karlsruhe, 1998.
- [4] Gonzalez *et al.*, *High energy flux measurements and high energy neutron studies (^3He ionisation, fission measurements, $(n,2n)$ reactions on ^{12}C and ^{232}Th and temperature measurements)*. Workshop on P&T strategy studies and transmutation experiments. Karlsruhe, 1998.
- [5] Arnould *et al.*, *Experimental Verification of Neutron Phenomenology in Lead and Transmutation by Adiabatic Resonance Crossing in Accelerator Driven Systems*. Submitted to Physics Letters on Dec. 1998.
- [6] Bergmann *et al.*, Proceedings 1st Int. Conf. Peaceful Uses At. Energy, 4,135 (1955). L.E. Lazareva *et al.*, J.E.T.P. 29,381 (1955)
- [7] F. Carminati *et al.*, TARC General Purpose Monte Carlo, CERN/LHC/EET 96-011, (1996).
- [8] The TARC Collaboration, Neutron Driven Nuclear Transmutation by Adiabatic Resonance Crossing. To be submitted to Nucl. Instrum. and Meth. (1999)
- [9] The TARC Collaboration, Final Report of Contract F141-CT96-009 of the EU in the 4th Framework Program. Neutron Driven Nuclear Transmutation by Adiabatic Resonance Crossing. In preparation.
- [10] Abanades *et al.*, *^{99}Tc Capture Rate Measurements with Spallation Neutrons in a Large Lead Block*. CERN/ET/Internal Note 97-14, (1997).
- [11] Chou and H. Werle, J. Nucl. Energy, 27,811. (1973).
- [12] Hopke *et al.*, Phys. Rev. C8 (1973).
- [13] BNL 325 Report on ^{129}I neutron capture cross-section (1973).
- [14] Andriamonje *et al.*, *Measurement of the Neutron Capture Rate on ^{127}I and ^{129}I with the TARC Experiment*. CERN/ET/Internal Note (1997).